

A New Two-dimensional Starved Lubrication Model for Studying Lubricant Transfer Effects of Surface Texture

Ke Zhang, Kazuyuki Yagi

Kyushu University

1. Introduction

Starved lubrication is commonly founded in piston rings and rolling bearings. The limited lubricant supply inhibits the generation of pressure and hence results in the reduction of film thickness and high friction. Experimental [1,2] studies show that textured surfaces can improve tribological performance by transferring lubricant oil stored in textured patterns to the inlet region, but numerical studies fail to predict the phenomenon well. There are two problems on the numerical model when simulating starvation with a textured surface. The first one is that the mass conservation of flow between the outside and the inside of the lubricated area should be considered. The second is that the advection term of the lubricant oil flow is usually solved with a low-order scheme to ensure computational stability, which is adverse to modeling the lubricant transport phenomenon.

In this study, a new two-dimensional model with a physically realistic free boundary condition and high-accuracy calculation algorithm is proposed for starved lubrication problems. The proposed model considers the mass conservation of flow between lubricant oil with a free surface outside the lubricated area and that inside the lubricated area. The CIP method is employed to solve the advection equation with high accuracy. It was found that the proposed model differed from the conventional Elrod-Adams model and had better solutions. Numerical results show that the tribology performance is improved by surface textures and demonstrates the great potential to further tailor textures for obtaining a better-lubricated condition.

2. Mathematical model

Figure 1 a two-dimensional model for starved lubrication with a textured surface. The pin is stationary, and the flat surface moves at a constant sliding speed u . Dimples with a radius r_d are located on the moving surface. Dimples are lined with a pitch d on the central line along the sliding direction. Lubricant oil with an initial thickness h_s is distributed on the moving surface. The boundary conditions for the calculation domain are also shown in Fig. 1. Table 1 shows detailed parameters for numerical simulation. The lubricant oil film in the calculation domain is divided into two regions. In the fully-filled region, the hydrodynamic pressure is generated and governed by the Reynolds equation. In the partially-filled region, the lubricant oil film adheres on the moving surface and has a free surface. The lubricant oil flow is governed by an advection equation without consideration of the surface tension and body force. In the conventional Elrod-Adams model, a unified Reynolds equation can be used for the whole calculation domain, as the mass transport speed is assumed to be constant between inside and outside the contact area. However, lubricant oil adheres mainly to the lower surface after film rupture in starved lubrication, and the mass transport speed should be the same as the speed of the moving surface [3]. Considering these physical conditions, a new model based on previous work [4] is used and extended to two dimensions to predict the flow of lubricant oil. The governing equation of the lubricant oil film is given as follows:

$$\frac{\partial}{\partial x} \left(h^3 \frac{\partial p}{\partial x} \right) + \frac{\partial}{\partial y} \left(h^3 \frac{\partial p}{\partial y} \right) = 12\mu U \frac{\partial(\alpha\theta h)}{\partial x} + 12\mu \frac{\partial(\theta h)}{\partial t} \quad (1)$$

where saturation variable θ is defined as the ratio of the film thickness to the local gap. Based on the previous study, the transport velocity parameter α was governed by,

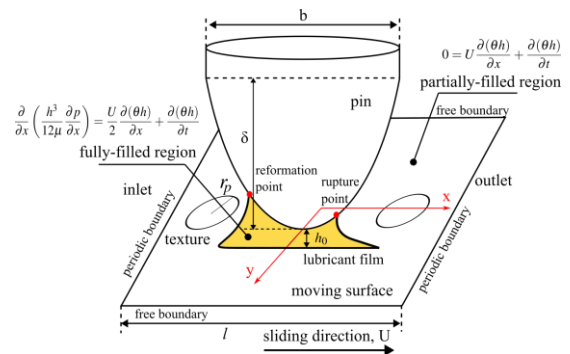


Fig. 1 Schematic of the piston/ring-liner system with textured surface at $T = 0$

Table 1 Simulation parameters

Parameters	Value
Calculation zone, l	1 mm
Pin width, b	1 mm
Pin height, σ	16 μm
Dimple radius, r_d	100 μm
Dimple depth, h_d	3 μm
Dimple pitch, d	1 mm
Initial lubricant supply, h_s	1.5 μm
Sliding speed, U	1 m/s
Minimum film thickness, h_0	1 μm
Viscosity, μ	0.01 Pas

$$\alpha_i = \begin{cases} 1, & \text{when } i \text{ in partially-filled region} \\ 1/\max(2\theta, 1), & \text{when } i \text{ in transition region} \\ 0.5, & \text{when } i \text{ in fully-filled region} \end{cases} \quad (2)$$

The free boundary of lubricants around the pin is updated by tracing the movement of the reformation and rupture points. To solve the above governing equations with high accuracy, the CIP-CSL2 [5] method is used, and the fractional step technique [6] is adopted to handle the two dimensions problems. The solution process can be simplified to:

Step 1 CIPCSLID($\alpha, f^n, f^{step1}, \sigma_x^n, \sigma_x^{step1}, x$)s

Step 2 Non – advection part

where $f = h\theta$ and the initial value of σ_x is $(f_{i,j} + f_{i-1,j}) / 2$.

3. Results and discussion

Figure 2 compares the simulation results of the conventional Elrod-Adams and the proposed model with experimental results [1]. In the experimental results [1], it was clear that a dimple filled with lubricant oil entered the contact area, and after passing through the contact area, a part of lubricant oil stored in the dimple was transferred to the moving surface. The transferred lubricant oil to the moving surface is believed to improve the supply of lubricant oil at the inlet region during the next contact, thus improving the tribological performance. In numerical results, the conventional Elrod-Adams model predicts that the lubricant oil stored in dimples has been transferred to the moving surface before entering the contact area as shown at $T = 0.2$ and 0.36 while there is no transferred lubricant oil remaining on the moving surface after the dimple passes through the contact area. The reason for this incorrect prediction is that the conventional Elrod-Adams model uses a uniform mass transport speed for lubricant oil flow in both the fully-filled and partially-filled regions. As a dimple passes through the reformation and rupture boundaries, it can cause mass conservation problems. Therefore, it is not possible to accurately capture the lubricant oil flow near dimples. On the other hand, at $T = 0.6$, the proposed model predicts that the rupture boundary is extended due to the dimple, and the lubricant stored in the dimple is gradually transferred to the moving surface. At $T = 0.71$, a considerable amount of lubricant oil has been transferred to the moving surface. The numerical results indicate the same transport process of lubricant oil as the experimental results [1].

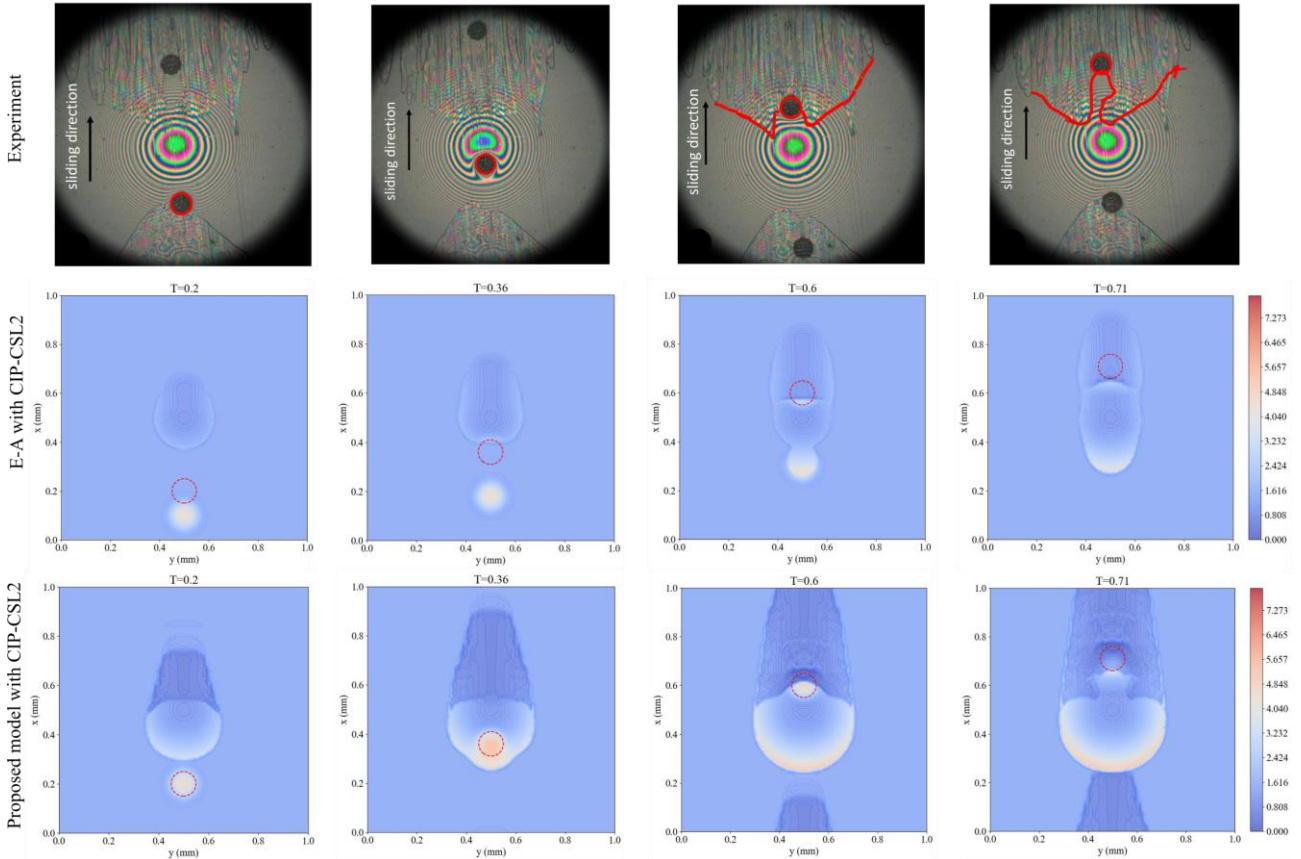


Fig. 2 Comparison of simulation results with experimental results

The above analysis shows that the proposed model in this study differs from the conventional model in the prediction of lubricant oil film distribution. Figure 3 shows variations in load-carrying capacity in the flat case for the proposed model and conventional model. Figure 4 shows a comparison in load carrying-capacity between the flat case and textured surface case with

a large computational domain. In the flat case, it can be seen that the proposed model gives a larger load-carrying capacity. It is because the proposed model reconstructs the mass conservation of flow between the inside and outside of the contact area. The mass transport speed in the partially-filled region is larger than in the Elrod-Adams model. Therefore, more lubricant accumulates near the inlet boundary, generating a higher hydrodynamic pressure.

In the textured surface case, the load-carrying capacity fluctuates largely because of dimples entering the contact area. The load-carrying capacity is not improved compared to the flat case at the early stage of the result. However, as time increases, the lubricant oil near the inlet region moves to the sidebands of the contact area. The inability to replenish the inlet lubricant oil leads to a gradual loss of load-carrying capacity and severe starvation. In contrast, the lubricated condition of the inlet region is well maintained in the textured surface case because dimples can gradually transfer the stored lubricant oil to the moving surface, as shown in Figure 4. The hydrodynamic pressure can be generated continuously, preventing the loss of load-carrying capacity. Better tribological performance can be obtained compared to the flat case.

4. Conclusions

This study proposed a new two-dimensional model for starved lubrication with texture surfaces. Compared with the conventional Elrod-Adams model, the current model successfully captures the lubricant transport phenomena, as shown in the experimental results. It numerically demonstrates that dimples can enhance tribological performance as the transferred lubricant prevents the aggravation of starvation. The proposed model is expected to guide the optimal design of textured patterns considering lubricant transport phenomena.

References

- 1) K. Ueda, K. Yagi & J. Sugimura: Lubricant Supply Action of Textured Surfaces in Starvation Conditions, トライボロジー会議 2018 春 東京, (2018) A11.
- 2) K. Yagi, W. Matsunaka & J. Sugimura: Impact of Textured Surfaces in Starved Hydrodynamic Lubrication, Tribol. Int., 154 (2020) 106756.
- 3) G. C. Buscaglia, I. Ciuperca, E. Dalissier & M. Jai: A New Cavitation Model in Lubrication: the Case of Two-Zone Cavitation, Journal of Engineering Mathematics, 83 (2013) 57–79.
- 4) K. Zhang, K. Yagi & J. Sugimura: Numerical Simulation on Lubricant Transport Mechanism of Surface Textures in Starved Hydrodynamic Lubrication, トライボロジー会議 2021 春 東京, (2021) A31.
- 5) T. Yabe, R. Tanaka, T. Nakamura & F. Xiao: An Exactly Conservative Semi-Lagrangian Scheme (CIP-CSL) in One Dimension, Monthly Weather Review, 129, 2 (2001) 332.
- 6) T. Nakamura, R. Tanaka, T. Yabe & K. Takizawa: Exactly Conservative Semi-Lagrangian Scheme for Multi-dimensional Hyperbolic Equations with Directional Splitting Technique, Journal of Computational Physics 174 (2001) 171–207.

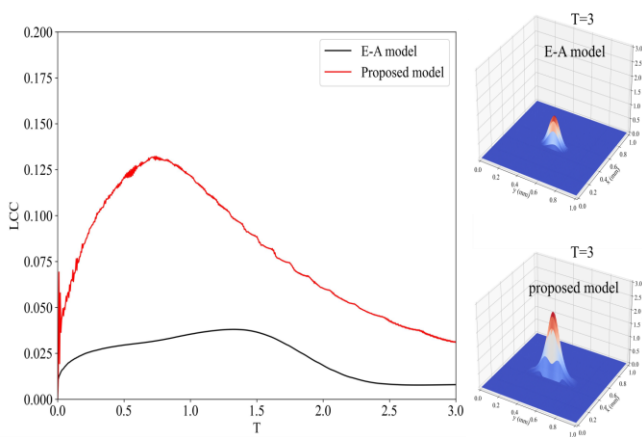


Fig. 3 Comparison of load-carrying capacity and pressure in flat cases between E-A model and proposed model

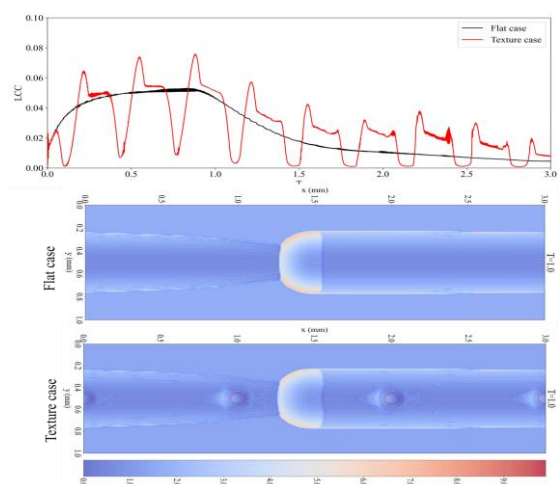


Fig. 4 Comparison of load-carrying capacity and film distributions between flat case and textured surface case